IL NUOVO CIMENTO Vol. 36 C, N. 6 Novembre-Dicembre 2013
DOI 10.1393/ncc/i2014-11638-1

Colloquia: LaThuile13

Diboson physics at ATLAS

K. Bachas on behalf of the ATLAS Collaboration

Aristotle University of Thessaloniki - Nuclear and Particle Physics Laboratory
54124 University Campus, Thessaloniki, Greece

ricevuto il 20 Giugno 2013; approvato l'1 Luglio 2013

Summary. — This paper is intended to give an overview of the ATLAS results on the production cross sections of gauge boson pairs in their fully leptonic decay modes using data from pp collisions at $\sqrt{s} = 7\,\text{TeV}$ for $W\gamma, Z\gamma, WW, ZZ$ and WZ and $\sqrt{s} = 8\,\text{TeV}$ for ZZ at the Large Hadron Collider. The cross sections are found to be in agreement with the expectation from the Standard Model within the estimated uncertainties. The production cross section measurements also allow for studies of anomalous triple gauge couplings for which 95% confidence limits are set.

PACS 14.70.-e – Gauge bosons.

1. – Introduction

Measurements of vector boson pair production provide excellent tests of the electroweak sector of the Standard Model (SM). In the SM, Triple Gauge Couplings (TGC) are predicted at tree level only with charged bosons, while neutral ones are forbidden. The TGC vertex is completely fixed by the electroweak gauge structure and so a precise measurement of this vertex, through the analysis of diboson production, is essential to test the high energy behavior of electroweak interactions and to probe for possible new physics in the bosonic sector. Any deviation from gauge constraints can cause a significant enhancement in the production cross section at high diboson invariant mass due to anomalous triple gauge boson couplings (aTGC).

This note presents measurements of the diboson production cross sections in proton-proton collisions and limits on aTGC with the ATLAS experiment [1]. The following diboson pair final states were investigated: $W\gamma, Z\gamma, WW, ZZ$ and WZ. A sample of integrated luminosity $L = 4.6\,\text{fb}^{-1}$ of 2011 data at a center of mass energy $\sqrt{s} = 7\,\text{TeV}$ was used for all diboson pair final states, while $L = 5.8\,\text{fb}^{-1}$ of 2012 data at $\sqrt{s} = 8\,\text{TeV}$ was also used for ZZ. All studies used the fully leptonic decay final states with $Z \to ll$ and $W \to l\nu$, where $l = e$ or μ. The studies of $Z\gamma$ and ZZ channels also considered $\nu\nu\gamma$ and $ll\nu\nu$ final states respectively.

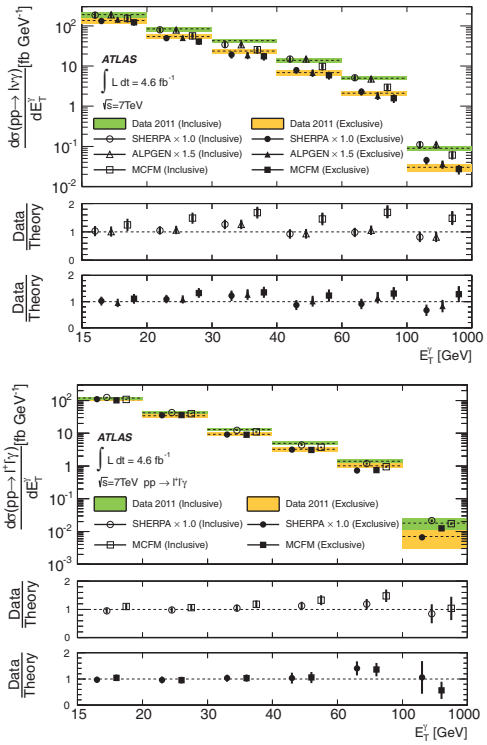

Fig. 1. – Measured E_T^γ differential cross sections of the $pp \to l\nu\gamma$ (left) and $pp \to ll\gamma$ (right) processes, using the combined electron and muon measurements in the inclusive ($N_{\text{jet}} \geq 0$) and exclusive ($N_{\text{jet}} = 0$) fiducial regions. The lower panes show the ratio of the data to the predictions by different generators. The Monte Carlo uncertainties are shown only in the ratio plots [2].

2. – $W\gamma$ and $Z\gamma$ cross section measurements

The diboson candidate events are selected from the production processes $pp \to l\nu\gamma + X$, $pp \to ll\gamma + X$ and $pp \to \nu\nu\gamma + X$. These final states include the production of W and Z bosons in association with photons from QED final State Radiation off the charged leptons, photons radiated from initial-state quarks, photons from the fragmentation of secondary quarks and gluons, and photons radiated by W bosons [2]. Two sets of cross section measurements are performed, namely the inclusive and exclusive, depending on the number of jets in the final state. The inclusive cross section measurement refers to production with no restriction on the recoil system. The exclusive measurement refers to events where no central jets with transverse energy $E_T > 30\,\text{GeV}$ are produced. Jets are reconstructed from energy observed in the calorimeter cells using the anti-kt jet clustering algorithm [3].

The experimental signature comprises a highly energetic isolated photon with $E_T^\gamma > 15\,\text{GeV}$ plus missing transverse energy of $E_T^{miss} > 35\,\text{GeV}$ for $l\nu\gamma$ or two oppositely charged same-flavor leptons with an invariant mass greater than 40 GeV for $ll\gamma$. For the $\nu\nu\gamma$ the requirements are $E_T^\gamma > 100\,\text{GeV}$ and $E_T^{miss} > 90\,\text{GeV}$. In order to suppress Final State Radiation (FSR) contribution, the angular separation between the lepton and the photon is required to be $\Delta R(l, \gamma) > 0.7$.

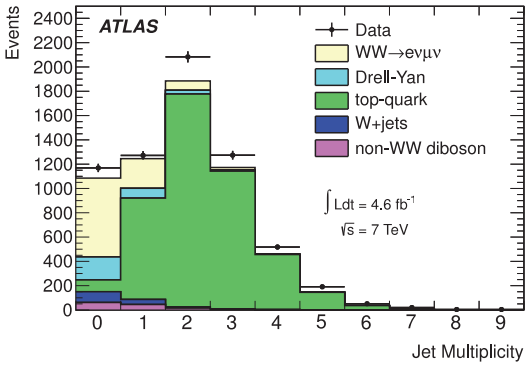

Fig. 2. – Jet multiplicity distribution of the $e\mu$ topology from data and Monte Carlo simulation [4].

The dominating background processes are Z+jets, W+jets and γ+jets but there are also contributions from $t\bar{t}$ and WW. On fig. 1 the measured E_T^{γ} differential cross sections for $pp \to W\gamma \to l\nu\gamma$ (left) and $pp \to Z\gamma \to ll\gamma$ (right) are shown for both the inclusive and exclusive measurements. It is evident that Alpgen and Sherpa generators describe the $W\gamma$ and $Z\gamma$ distributions in data quite well for both topologies. The inclusive $W\gamma$ measurement is underestimated by MCFM generator. The likely cause is the missing higher-order QCD contributions beyond the available NLO prediction. On the other hand for $Z\gamma$ the agreement is quite good.

The systematic uncertainties on the cross sections are dominated by effects coming from the photon identification, background subtraction and jet energy scale uncertainties.

3. – WW cross section measurement

The $WW \to l\nu l\nu$ signal is measured in final states with two oppositely charged isolated leptons and large missing transverse energy [4]. The minimum requirement on the p_T of the leptons is 25 GeV while for the missing transverse energy the $E_{T,Rel}^{miss}$ variable is used, defined as:

$$E_{T,Rel}^{miss} = \begin{cases} E_T^{miss} \times \sin(\Delta\phi), & \text{if} \quad \Delta\phi < \pi/2, \\ E_T^{miss}, & \text{if} \quad \Delta\phi \geq \pi/2, \end{cases} \tag{1}$$

where $\Delta\phi$ is the difference in the azimuthal angle between the E_T^{miss} direction and the nearest lepton or jet in the plane transverse to the beam. For the $ee, \mu\mu$ and $e\mu$ topologies the minimum $E_{T,Rel}^{miss}$ requirement is 45, 45 and 25 GeV respectively. Figure 2 shows the jet multiplicity distribution of the $e\mu$ topology. Candidate WW events are required to have no jets reconstructed in the final state.

Processes that can mimic the $ll + E_T^{miss}$ signal with no reconstructed jets are the top-quark production when additional jets in the final state fail reconstruction, W+jets when a jet fakes a lepton, Drell-Yan with mismeasured jets, WZ and ZZ processes when only two leptons are reconstructed in the final state, and the $W\gamma$ process when the photon converts into electrons.

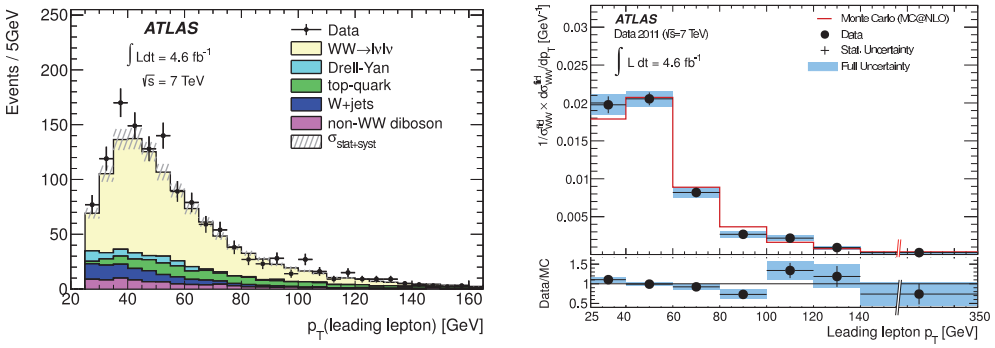

Fig. 3. – Left: Leading lepton p_T distribution for WW candidates with all selection criteria applied and combining ee, $\mu\mu$ and $e\mu$ channels. Background contributions from the Drell-Yan, top-quark and W+jets processes are obtained from data-driven methods. The prediction of the SM WW contribution is normalized to the inclusive theoretical cross section of 44.7 pb [4]. Right: Normalized fiducial cross section together with the overall uncertainty in bins of the leading lepton p_T.

After applying the selection criteria 1325 events are observed and the total estimated background is $369 \pm 31(\text{stat.}) \pm 53(\text{syst.})$ events, extracted from data-driven and MC based methods. The left distribution of fig. 3 shows the comparison of data and MC of the leading lepton p_T after all selection criteria are applied, while the one on the right shows the normalized fiducial cross section in bins of leading lepton p_T.

The measured total production cross section is $51.9 \pm 2.0(\text{stat.}) \pm 3.9(\text{syst.}) \pm 2.0(\text{lumi.})$ pb while the theoretical prediction gives $44.7^{+2.1}_{-1.9}$ pb. The driving uncertainty of the measurement is the systematics due to the jet veto requirement and the estimation of fake lepton backgrounds.

4. – ZZ cross section measurement

The analyses of Z boson pair production is performed in the $4l$ and $2l2\nu$ final states [5]. In the former topology the signature comprises of 4 isolated leptons with p_T starting from 7 GeV and the invariant mass of each reconstructed lepton pair is required to be in the mass window $[66, 116]$ GeV. For the latter topology, the signature is 2 high-p_T isolated leptons and axial-$E_T^{miss} > 75$ GeV, where the axial-E_T^{miss} is the projection of E_T^{miss} along the opposite direction of the Z. The invariant mass of the two leptons should lie in the window $[76, 106]$ GeV. Note that for the fiducial cross section results the ZZ^* case is also considered, where the invariant mass of the subleading lepton pair should be more than 20 GeV. In the left plot of fig. 4 the mass of the leading lepton pair *versus* the mass of the sub-leading lepton pair, is given. The right plot of fig. 4 shows the invariant mass of the 4-lepton system in the ZZ^* selection.

The $4l$ final state is a very clean signature with small background contributions. These mainly come from Z+jets and $t\bar{t}$ processes where the jets are misidentified as leptons and they are estimated with data-driven methods. The background is more significant in the $2l2\nu$ final state and is a mixture of diboson, $t\bar{t}$ and Drell-Yan events.

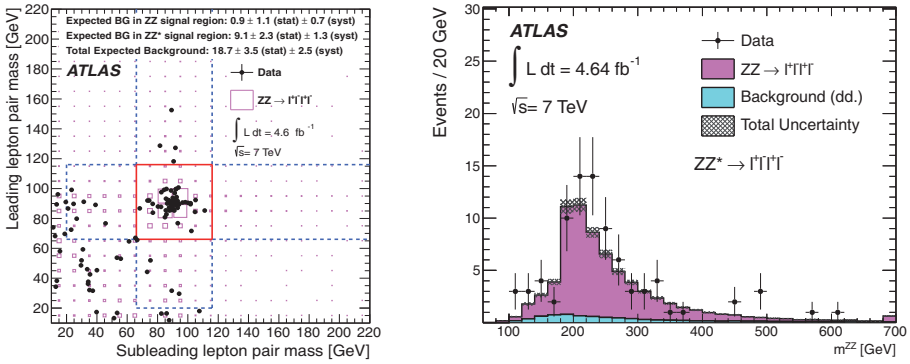

Fig. 4. – Left: The mass of the leading lepton pair *versus* the mass of the sub-leading lepton pair. The events observed in data are shown as solid circles and the $ZZ^* \to llll$ signal prediction from simulation as boxes. The size of each box is proportional to the number of events in each bin. The region enclosed by the solid (dashed) lines indicates the signal region defined by the requirements on the lepton-pair masses for ZZ (ZZ^*) events. Right: Invariant mass of the 4-lepton system for the ZZ^* selection. The points represent data and the histograms show the prediction from simulation, where the background is normalized to the data-driven estimate. The shaded band shows the combined statistical and systematic uncertainty on the prediction [5].

After all event selections are applied, the observed yield in the $4l$ final state is 66 (84) events in the ZZ (ZZ^*) case with a background expectation of $0.9 \pm 1.1(\text{stat.}) \pm 0.7(\text{syst.})$ $(9.1 \pm 2.3(\text{stat.}) \pm 1.3(\text{syst.}))$. The corresponding yield for the $2l2\nu$ final state is 87 events with background expectation of $46.9 \pm 4.8(\text{stat.}) \pm 1.9(\text{syst.})$. The total production cross section is measured in both 7 TeV and 8 TeV data, in the case where both Z bosons are on-shell. The results are summarized in fig. 5. For 7 TeV the total cross section is

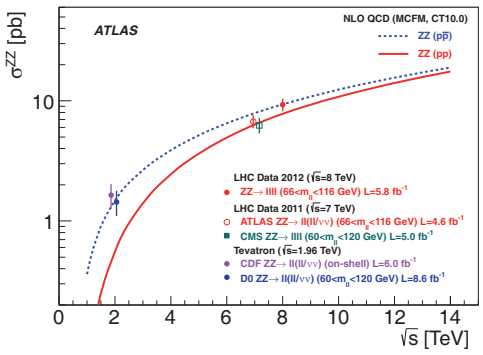

Fig. 5. – Measurements and theoretical predictions of the total ZZ production cross section as a function of the center-of-mass energy $\sqrt{s}$. Experimental measurements from CDF and D0 in $p\bar{p}$ collisions at the Tevatron at $\sqrt{s} = 1.96\,\text{TeV}$, and experimental measurements from ATLAS in pp collisions at the LHC at $\sqrt{s} = 7\,\text{TeV}$ and $\sqrt{s} = 8\,\text{TeV}$ are shown. The blue dashed line shows the theoretical prediction for the ZZ production cross section in $p\bar{p}$ collisions. The solid red line shows the theoretical prediction for the ZZ production cross section in pp collisions [6].

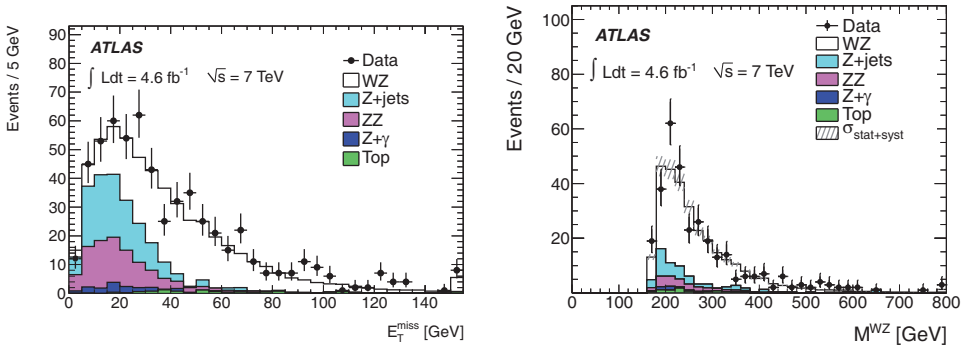

Fig. 6. – Left: Data and MC comparison of the E_T^{miss} distribution in trilepton events before applying the E_T^{miss} requirement. Right: Invariant mass m_{WZ} of the WZ pair. The shaded bands indicate the total statistical and systematic uncertainties of the prediction. For Z+jets and $t\bar{t}$, the expected shape is taken from simulation but the normalization is taken from the data-driven estimates. The rightmost bins include overflow [7].

$6.7 \pm 0.7(\text{stat.})^{+0.4}_{-0.3}(\text{syst.}) \pm 0.3(\text{lumi.})$ pb with theoretical prediction of $5.89 \pm^{+0.22}_{-0.18}$ pb. For 8 TeV the total cross section is $9.3^{+1.1}_{-1.0}(\text{stat.})^{+0.4}_{-0.3}(\text{syst.}) \pm 0.3(\text{lumi.})$ pb with theoretical prediction $7.4^{+0.4}_{-0.4}$ pb [6]. The main uncertainty of the measurement is statistical while the systematic uncertainty with the greatest contribution is the lepton reconstruction and isolation efficiency.

5. – WZ cross section measurement

The analysis of WZ production is performed with $3l\nu$ final states [7]. The signature of these topologies is 3 high-p_T isolated leptons with $p_T > 15, 15, 20$ GeV for the two leptons from Z and the one from the W respectively, and $E_T^{miss} > 25$ GeV.

Main sources of background are the Z+jets and $t\bar{t}$ events where the two leptons from the vector boson decays are accompanied by a jet which is misidentified as a lepton. These backgrounds are estimated from data-driven techniques. There is also contribution from ZZ background where one lepton falls outside the acceptance of the detector and thus creates E_T^{miss}. This source is estimated from MC. In fig. 6 the E_T^{miss} (left) and the invariant mass of the WZ system (right) are shown.

The presence of 3 leptons in the final state and the requirement of a tight invariant mass window for the Z leptons around the Z pole ($|m_Z - m_{PDG}| < 10$ GeV) suppresses significantly the background. Imposing stricter selection criteria for the W lepton with respect to the leptons coming from the Z boson, suppresses the background coming from Z+jets and $t\bar{t}$ even further.

Given the selection requirements, the total number of observed events is 317 with a background expectation of 68 ± 10 events. Figure 7 shows the normalized fiducial cross section in bins of p_T^Z (left) and m_{WZ} (right) compared to the SM prediction. The measured total production cross section is $19.0^{+1.4}_{-1.3}(\text{stat.}) \pm 0.9(\text{syst.}) \pm 0.4(\text{lumi.})$ pb while the expectation from SM is $17.6^{+1.1}_{-1.0}$ pb.

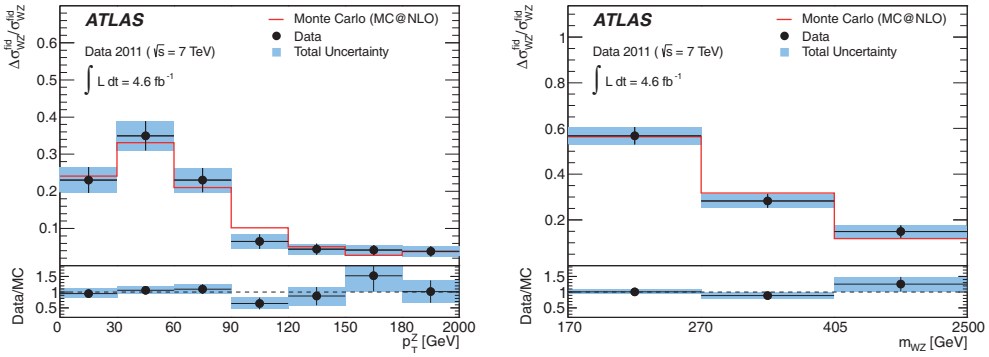

Fig. 7. – Normalized fiducial cross section in bins of p_T^Z (left) and m_{WZ} (right) compared to the SM prediction. The total uncertainty contains statistical and systematic uncertainties added in quadrature [7].

6. – Triple Gauge Couplings measurements

The effect of aTGC is modelled using an effective Lagrangian which depends on the parameters shown in table I [8, 9]. If aTGCs exist they are expected to modify the production rates and kinematics of the processes which would manifest as enhanced production cross sections at high invariant mass and high-p_T. Neutral aTGC are not allowed in the SM which predicts all parameters to be zero except for the charged aTGC parameters g_1^V and κ^V which are 1. In figs. 8 and 9 a summary of the limits set on the different aTGC parameters is shown along with comparisons to other experiments. Figure 8 shows limits set by the $W\gamma$, $Z\gamma$ and WW analyses described before, while limits illustrated in fig. 9 are extracted from the ZZ and WZ analyses. No deviation from the expected SM values is observed in any channel.

TGC limits from WW analysis approach the precision of the combination limits from LEP experiments. Because of the higher energy and production cross section at the LHC, limits are better than the Tevatron. Limits from ZZ analysis are significantly tighter than the LEP and D0 experiments. Limits from $W\gamma$ analysis are looser than the ones set from LEP and D0. Finally, the aTGC limits from WZ analysis set on Δg_1^Z and λ_Z are tighter than Tevatron while for $\Delta\kappa_Z$ approaches Tevatron's precision.

TABLE I. – *List of TGC parameters that enter in the effective Lagrangian for each diboson process.*

Interaction	Parameters	Channel
$WW\gamma$	λ_γ, $\Delta\kappa_\gamma$	WW, $W\gamma$
WWZ	λ_Z, $\Delta\kappa_Z$, Δg_1^Z	WW, WZ
$ZZ\gamma$	h_3^Z, h_4^Z	$Z\gamma$
$Z\gamma\gamma$	h_3^γ, h_4^γ	$Z\gamma$
$Z\gamma Z$	f_{40}^Z, f_{50}^Z	ZZ
ZZZ	f_{40}^γ, f_{50}^γ	ZZ

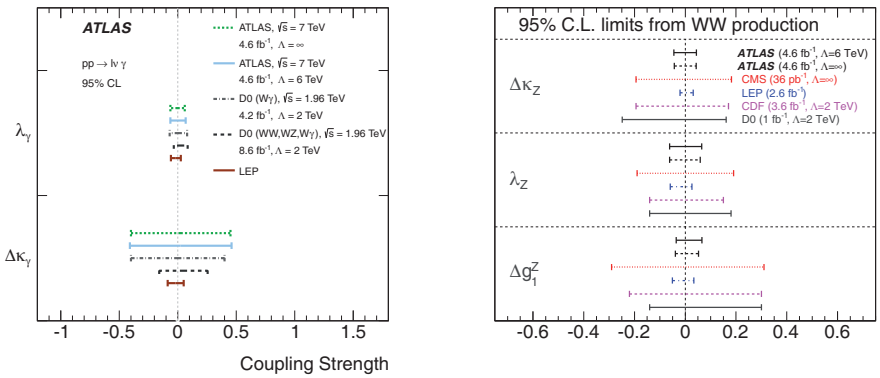

Fig. 8. – Left: 95% CL intervals for anomalous couplings from ATLAS, D0 and LEP for the charged aTGCs $\Delta\kappa_\gamma$ and λ_γ. The ATLAS and D0 results from $W\gamma$ production are shown. The LEP charged aTGCs results were obtained from WW production, which is also sensitive to the WWZ couplings. The combined aTGC results from D0 were obtained from $WW+WZ \to l\nu jj$, $WW+WZ \to l\nu ll$, $W\gamma \to l\nu\gamma$ and $WW \to l\nu l\nu$ events. The integrated luminosities and cut-off parameter Λ are shown. Except for the coupling under study, all other anomalous couplings are set to zero. Right: Comparison of aTGC limits from ATLAS, CMS, CDF, D0 and LEP experiments for the $\Delta\kappa_Z$, λ_Z and Δg_1^Z using WW events [2, 4].

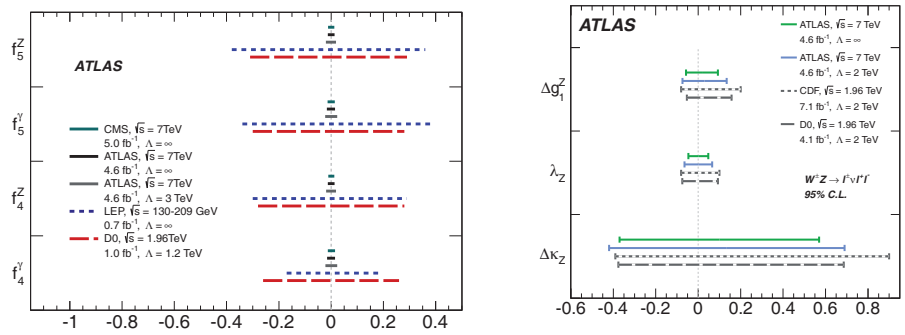

Fig. 9. – Left: Anomalous TGC 95% confidence intervals from ATLAS, CMS, LEP and Tevatron experiments using ZZ events. Right: Anomalous TGC limits at 95% confidence level from ATLAS, CDF, and D0 obtained from WZ production. Integrated luminosities, centre-of-mass energy and cut-off Λ for each experiment are shown on both plots [5, 7].

7. – Conclusions

Measurements of the production cross sections of $W\gamma$, $Z\gamma$, WW, ZZ and WZ have been performed with the ATLAS detector at center-of-mass energy $\sqrt{s} = 7\,\text{TeV}$ with 2011 LHC data and at $\sqrt{s} = 8\,\text{TeV}$ with 2012 data for ZZ. The total production cross sections are compatible with the SM expectations within uncertainties. No evidence for new physics is observed from the kinematic distributions of the diboson processes. Limits on anomalous triple gauge couplings are set in all channels and values of aTGC parameters are well within the SM predictions.

* * *

This research has been co-financed by the European Union (European Social Fund ESF) and Greek national funds through the Operational Program "Education and Lifelong Learning" of the National Strategic Reference Framework (NSRF) - Research Funding Program: Thales. Investing in knowledge society through the European Social Fund.

REFERENCES

[1] ATLAS Collaboration, *JINST*, **3** (2008) S08003.
[2] ATLAS Collaboration, arXiv:1302.1283v1 [hep-ex].
[3] Cacciari M., Salam G. P. and Soyez G., *JHEP*, **04** (2008) 063.
[4] ATLAS Collaboration, arXiv:1210.2979v1 [hep-ex].
[5] ATLAS Collaboration, *JHEP*, **03** (2013) 128.
[6] ATLAS Collaboration, ATLAS-CONF-2012-090, `https://cds.cern.ch/record/1460409`.
[7] ATLAS Collaboration, *Eur. Phys. J. C*, **72** (2012) 2173.
[8] Hagiwara K. *et al.*, *Nucl. Phys. B*, **282** (1987) 253.
[9] Ellison J. *et al.*, *Annu. Rev. Nucl. Part. Sci.*, **48** (1998) 33.